ELSEVIER

www.elsevier.nl/locate/jorganchem

Journal of Organometallic Chemistry 611 (2000) 566–569

Journal of Organo metallic Chemistry

Self-assembled monolayers with oligo-ethyleneoxy linkages on flat and curved gold surfaces

Hidetaka Nakai, Hisashi Fujihara *

Department of Applied Chemistry, Kinki University, Kowakae, Higashi-Osaka 577-8502, Japan

Received 6 April 2000; accepted 18 April 2000

Abstract

The preparation and properties of the self-assembled monolayers with oligo-ethyleneoxy linkages on flat and curved gold surfaces have been described. The electrochemical properties of the self-assembled monolayers of a tetrathiafulvalenyl-alkane monothiol and the ether-substituted alkane monothiol adsorbed onto gold electrodes showed no difference in their redox potentials and surface coverages. In contrast, the difference between the alkyl chain and the oxy-alkyl chain in the redox potentials and surface coverages was found in the self-assembled monolayers of the tetrathiafulvalenyl-tetrathiol and the ether-substituted tetrathiol adsorbed onto gold electrodes. The reaction of a thiol bearing oligo-ethyleneoxy linkages with octanethiolate-stabilized gold clusters gave the new oxy-Au clusters containing ether linkages which were dissolved in nonpolar and polar solvents.

Keywords: Self-assembled monolayer; Gold cluster; Oligo-ethyleneoxy linkage; Electrochemical oxidation

1. Introduction

The self-assembly of molecules on metal surfaces has been the subject of intense interest. The spontaneous adsorption of long chain alkane-monothiols, e.g., $CH_3(CH_2)_nSH$, where $n = 8–16$, on flat or curved gold surface leads to the formation of self-assembled monolayers [1–4]. The intermolecular interactions in the self-assembled monolayers on flat or curved gold surface usually involve the hydrocarbon tails and are derived mainly from the van der Waals interactions. This fact has favored the use of organosulfur compounds with long chain alkane-monothiols, where $n > 8$, over compounds with shorter chains because short chain alkane-monothiols tend to form less stable. However, if the spacers were to be anchored to the metal surface by two or more attachment points, it is conceivable that the properties of electroactive monolayers might be controlled without dependence on the length of alkyl chains. As such an example, we reported that a tetrathiafulvalene (TTF) derivatized tetrathiol with four propyl chains forms the remarkably stable self-assembled monolayers, although the self-assembled monolayer of the TTF-monothiol with single propyl chain is unstable than that of the TTF-tetrathiol with four propyl chains [5]. Furthermore, we have shown that the TTF-alkanethiols adsorb onto curved gold surfaces and form the TTF-alkanethiolate monolayer-protected gold clusters [6].

Meanwhile, only limited studies using alkyl chains containing heteroatoms and functional groups in the self-assembled monolayers on flat and curved gold surfaces are reported [1–4]. This paper presents the preparation and characteristic properties of new self-assembled monolayers of tetrathiafulvalenyl-tetrathiol with oligo-ethyleneoxy linkages and a new class of gold clusters with oligo-ethyleneoxy linkages, and the differences in their properties between the alkyl chains and the oxy-alkyl chains.

2. Results and discussion

2.1. Self-assembled monolayers on flat gold surface

The electrochemical properties of alkane thiols (**1** and **2**) and ether-substituted alkane thiols (**1-O** and

---

* Corresponding author. Fax: + 81-6-67274301.
E-mail address: h-fuji@apch.kindai.ac.jp (H. Fujihara).

0022-328X/00/$ - see front matter © 2000 Elsevier Science S.A. All rights reserved.
PII: S0022-328X(00)00396-X

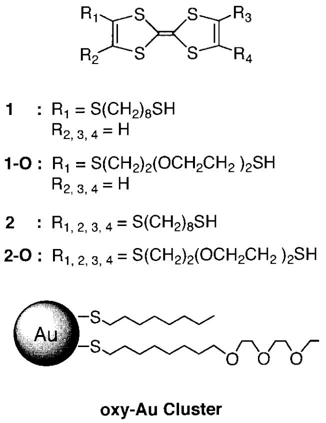

Chart 1.

2-O) in C_6H_5CN–0.1 M Bu_4NClO_4 at a glassy carbon electrode were studied by cyclic voltammetry (Chart 1). The cyclic voltammograms of the thiols (**1**, **1-O**, **2**, and **2-O**) showed the two reversible redox peaks at the following redox potentials ($E_{1/2}$ vs. Ag/0.1 M $AgNO_3$), **1**: +0.16 and +0.55 V, **1-O**: +0.16 and +0.54 V, **2**: +0.28 and +0.52 V, and **2-O**: +0.27 and +0.50 V. These data show no difference on the oxidation potentials between the alkane thiols and the ether-substituted alkane thiols.

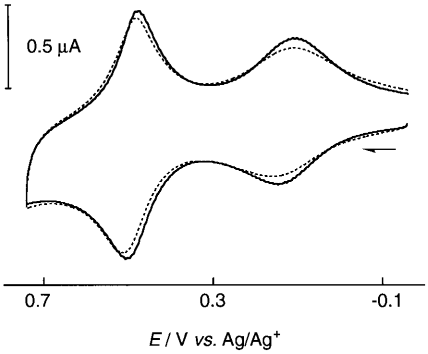

Fig. 1. Cyclic voltammograms for self-assembled monolayers of monothiols **1** (dotted line) and **1-O** (solid line) adsorbed onto gold electrodes in 0.1 M Bu_4NClO_4–CH_3CN; scan rate 100 mV s^{-1}.

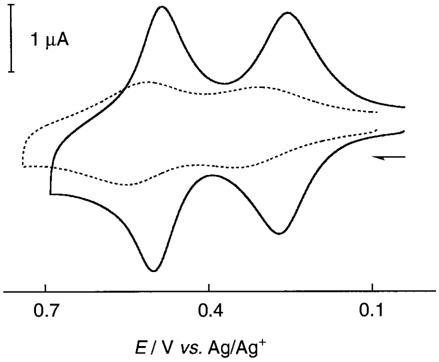

Fig. 2. Cyclic voltammograms for self-assembled monolayers of tetrathiols **2** (dotted line) and **2-O** (solid line) adsorbed onto gold electrodes in 0.1 M Bu_4NClO_4–CH_3CN; scan rate 100 mV s^{-1}.

Self-assembled monolayers (SAM) were formed by soaking gold electrodes in toluene solutions of the thiols (**1**, **1-O**, **2**, and **2-O**). After soaking for 20 h, the samples were removed, rinsed, and used for electrochemical studies in CH_3CN–0.1 M Bu_4NClO_4. The cyclic voltammograms of the self-assembled monolayers of monothiols **1** and **1-O** adsorbed onto gold electrodes in CH_3CN–0.1 M Bu_4NClO_4 exhibited the two reversible redox waves corresponding to the TTF–TTF^{+}–TTF^{2+} system at the following potentials ($E_{1/2}$ vs. Ag/0.1 M $AgNO_3$), **1-SAM**: +0.13 and +0.50 V, **1-O-SAM**: +0.13 and 0.50 V (Fig. 1). The surface coverages (Γ) of the self-assembled monolayers of monothiols **1** and **1-O** were 9.0×10^{-11} mol cm^{-2} for **1-SAM** and 9.5×10^{-11} mol cm^{-2} for **1-O-SAM**, respectively. These findings indicate no difference on the oxidation potentials and the surface coverages of the alkane monothiol **1-SAM** and the oxy-alkane monothiol **1-O-SAM**.

Interestingly, however, the difference between the alkane tetrathiol **2** and the oxy-alkane tetrathiol **2-O** was found in the corresponding self-assembled monolayers, i.e., the cyclic voltammograms for the self-assembled monolayers of tetrathiols **2** and **2-O** adsorbed onto gold electrodes in CH_3CN–0.1 M Bu_4NClO_4 showed the two reversible redox peaks at the following potentials ($E_{1/2}$ vs. Ag/0.1 M $AgNO_3$), **2-SAM**: +0.32 and +0.54 V, and **2-O-SAM**: +0.26 and +0.50 V (Fig. 2). Thus, the oxidation potentials of the oxy-tetrathiol **2-O-SAM** adsorbed onto a gold electrode were lower than those of the tetrathiol **2-SAM**. In the case of oxy-alkane tetrathiol SAM, the redox peaks shifted negatively by 60 mV. In order to explain the negative shift, we propose the following assumption based on the report that the redox peaks of the ferrocenylalkanethiol monolayer were strongly affected by the anion in solution [7]. The generated cationic species of the TTF units in the self-assembled monolayers may be stabilized by the counter anion (ClO_4^-) of the electrolyte which is located nearby at the ether units of **2-O-SAM** may interact with the ammonium cation of the electrolyte. Namely, this effect on the oxy-alkane tetrathiol SAM is bigger than that of the alkyl chains without ether groups. Analogously, such difference between alkyl chain and ether-substituted alkyl chain was observed in the surface coverages (Γ) of **2-SAM** and **2-O-SAM**, Γ of **2-SAM** $= 5.7 \times 10^{-11}$ mol cm^{-2} and Γ of **2-O-SAM** $= 3.0 \times 10^{-10}$ mol cm^{-2}. These results show that the interfacial properties of the self-assembled monolayers on flat gold surfaces can be controlled by the oligo-ethyleneoxy linkages.

2.2. Monolayer-protected gold clusters

New oxy-Au clusters were synthesized by the exchange reaction [8] of octanethiol-derivatized gold clus-

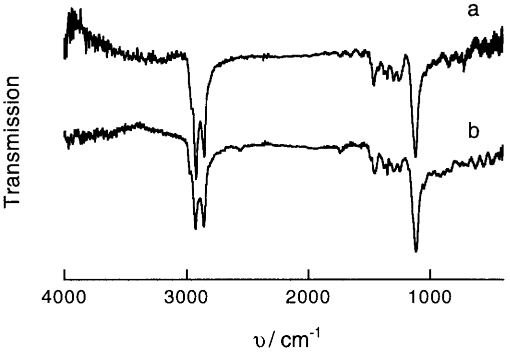

Fig. 3. IR spectra of (a) oxy-thiol and (b) oxy-Au clusters.

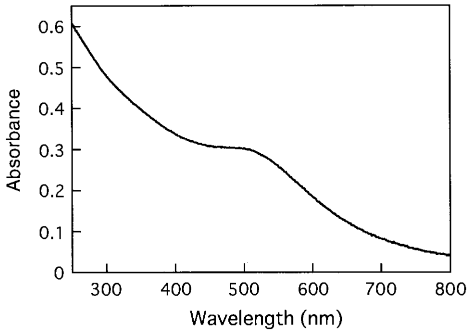

Fig. 4. UV spectrum of oxy-Au clusters.

ters [4] with an oxy-thiol [$HS(CH_2)_8(OCH_2CH_2)_2$-OC_2H_5]. Significantly, the new gold clusters containing oligo-ethyleneoxy linkages can be dissolved in methanol and ethanol. In contrast, the octanethiol-derivatized gold clusters can not be dissolved in methanol and ethanol.

The oxy-Au clusters were characterized by spectroscopic means. The FT-IR spectrum of the oxy-Au clusters (Fig. 3b) resembles that of the oxy-thiol (Fig. 3a) giving clear evidence that the oxy-thiol forms part of the composite. The UV–vis spectrum of the oxy-Au clusters in CH_2Cl_2 exhibited a plasmon resonance at 520 nm (Fig. 4). Fig. 5 shows the transmission electron microscopy (TEM) micrograph and size distribution of the oxy-Au clusters. The size range for oxy-Au clusters is found to be 3.6 ± 0.9 nm, compared with 3.3 ± 0.6 nm for the octanethiol-derivatized gold clusters as starting material. Thus we found that the property of the gold clusters can be changed by introduction of oligo-ethyleneoxy linkages.

3. Experimental

^1H- (270 MHz) and ^{13}C- (67.94 MHz) NMR spectra were recorded on a JEOL GSX270 spectrometer. UV spectra in solution were recorded with a HITACHI U-4000. FT-IR spectra were recorded with a PERKIN ELMER 1760-X. TEM micrographs were measured with a JEOL JEM 3010.

3.1. Synthesis of TTF-derivatives

New tetrathiafulvalenylthiols (**1**, **1-O**, **2**, and **2-O**) have been prepared as follows. The reaction of tetrathiafulvalene-monothiolate anion [9] with 8-iodooctyl thioacetate gave 4(8-thio-acetoxyoctylthio)tetrathiafulvalene which was then treated with $LiAlH_4$ to afford 4(8-mercaptoctylthio)tetrathiafulvalene (**1**). The reaction of a tetrathiafulvalene-tetrathiolate salt [10] with 8-iodooctyl thioacetate gave tetrakis(8-thioacetoxyoctylthio)tetrathiafulvalene which was treated with $LiAlH_4$ to afford tetrakis(8-mercaptoctylthio)tetrathiafulvalene (**2**). The use of 8-iodo-3,6-dioxaoctyl thioacetate, in place of 8-iodooctyl thioacetate, also resulted in formation of the ether-substituted thiols (**1-O** and **2-O**). **1**: FT-IR 2559 cm^{-1} (SH). ^1H-NMR ($CDCl_3$) δ 1.28–1.41 (m, 9H, CH_2, SH), 1.58–1.65 (m, 4H, SCH_2CH_2, CH_2CH_2SH), 2.52 (dt, 2H, $J = 7.6$, 7.0 Hz, CH_2SH), 2.74 (t, 2H, $J = 7.0$ Hz, SCH_2), 6.32 (s, 2H, C=CH), 6.33 (s, 1H, C=CH). ^{13}C-NMR ($CDCl_3$) δ 24.6, 28.2, 28.8, 28.9, 29.4, 33.9, 35.8, 109.8, 112.3, 118.9, 119.0, 121.8, 127.4. Exact mass calc. for

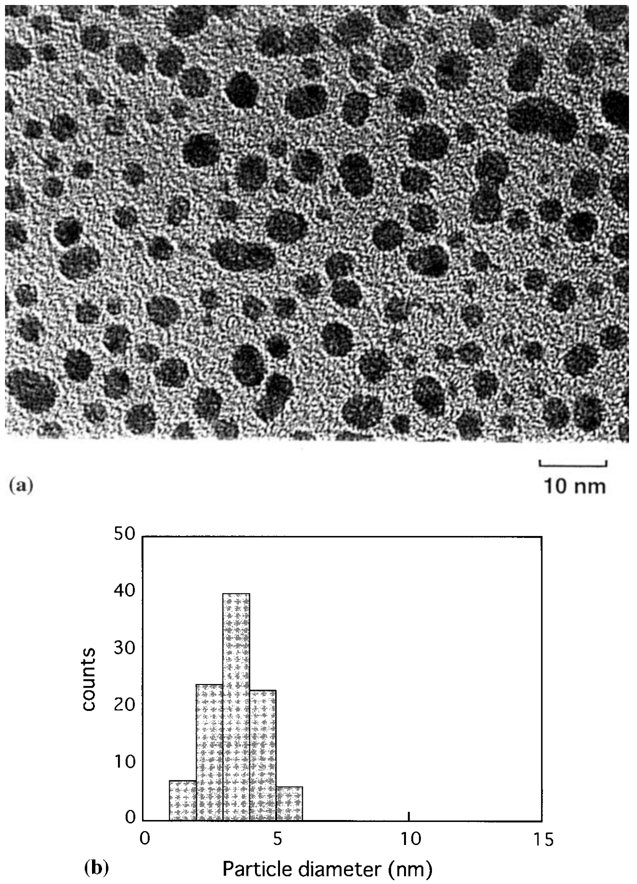

Fig. 5. (a) TEM micrograph and (b) size distribution of oxy-Au clusters.

$C_{14}H_{20}S_6$: 379.9890. Found: 379.9925. **1-O**: FT-IR 2559 cm^{-1} (SH). ^{1}H-NMR ($CDCl_3$) δ 1.58 (t, 1H, $J = 8.1$ Hz SH), 2.70 (dt, 2H, $J = 8.1$, 6.8 Hz, CH_2SH), 2.95 (t, 2H, $J = 6.8$ Hz, SCH_2), 3.61–3.64 (m, 6H, OCH_2), 3.69 (t, 2H, $J = 6.8$ Hz, SCH_2CH_2,O), 6.32 (s, 2H, C=CH), 6.41 (s, 1H, C=CH). ^{13}C-NMR ($CDCl_3$) δ 24.3, 35.1, 69.8, 70.2, 70.4, 72.9, 109.5, 112.9, 118.9, 119.0, 123.1, 126.5. Exact mass calc. for $C_{12}H_{16}O_2S_6$: 383.9475. Found: 383.9450. **2:** FT-IR 2559 cm^{-1} (SH). ^{1}H-NMR ($CDCl_3$) δ 1.29–1.44 (m, 36H, CH_2, SH), 1.58–1.66 (m, 16H, SCH_2CH_2, CH_2CH_2SH), 2.52 (dt, 8H, $J = 7.6$, 7.0 Hz, CH_2SH), 2.81 (t, 8H, $J = 7.0$ Hz, SCH_2). ^{13}C-NMR ($CDCl_3$) δ 24.6, 28.2, 28.4, 28.8, 28.9, 29.6, 33.9, 36.2, 109.9, 127.7. Exact mass calc. for $C_{38}H_{68}S_{12}$: 908.1970. Found: 908.1947. **2-O:** FT-IR 2559 cm^{-1} (SH). ^{1}H-NMR ($CDCl_3$) δ 1.60 (t, 4H, $J = 8.1$ Hz SH), 2.71 (dt, 8H, $J = 8.1$, 6.8 Hz, CH_2SH), 3.03 (t, 8H, $J = 6.8$ Hz, SCH_2), 3.62–3.66 (m, 24H, OCH_2), 3.69 (t, 8H, $J = 6.8$ Hz, SCH_2CH_2,O). ^{13}C-NMR ($CDCl_3$) δ 24.3, 35.5, 70.0, 70.2, 70.5, 72.9, 110.0, 127.9. Exact mass calc. for $C_{30}H_{52}O_8S_{12}$: 925.0311. Found: 924.0295.

3.2. Preparation of oxy-Au clusters

A solution of oxy-thiol [$HS(CH_2)_8(OCH_2CH_2)_2$-OC_2H_5; 15.0 mg, 0.043 mmol] and octanethiol-derivatized gold clusters (100 mg) in CH_2Cl_2 (50 ml) was stirred for 48 h at room temperature (r.t.). After stirring the organic phase was evaporated to 10 ml in vacuo and mixed with EtOH (1 ml)–H_2O (50 ml). The resulting precipitate was collected by filtration and washed serially with EtOH–H_2O (1:20). The oxy-Au clusters obtained were very stable and soluble in toluene, CH_2Cl_2, $CHCl_3$, MeOH, and EtOH.

3.3. Electrochemical measurements

All the electrochemical experiments were performed at r.t. using a BAS Instrument model 100B/W electrochemical workstation. Platinum wire was used as the counter electrode and glassy carbon (3.0 mm diameter) or gold (1.6 mm diameter) was used as the working electrode in a one-compartment cell. All potentials were relative to the system Ag/0.1 M $AgNO_3$ in acetonitrile. Bu_4NClO_4 and Bu_4NPF_6 (both Fluka, electrochemical grade), and CH_3CN and CH_2Cl_2 (both Wako, anhydrous) were used for the preparation of electrolyte solutions.

Acknowledgements

This work was supported in part by the grant-in-aid for Scientific Research on Priority Area (A) on 'The Chemistry of Inter-element Linkage' (nos. 09239252, 10133255 and 11120258) from the Ministry of Education, Science and Culture, Japan.

References

[1] A. Ulman, An Introduction to Ultrathin Organic Films, Academic Press, Boston, 1991.

[2] L.H. Dubois, R.G. Nuzzo, Annu. Rev. Phys. Chem. 43 (1992) 437.

[3] A. Ulman, Chem. Rev. 96 (1996) 1533.

[4] M. Brust, M. Walker, D. Bethell, D.J. Schiffrin, R. Whyman, J. Chem. Soc. Chem. Commun. (1994) 801.

[5] H. Fujihara, H. Nakai, M. Yoshihara, T. Maeshima, J. Chem. Soc. Chem. Commun. (1999) 737.

[6] H. Nakai, M. Yoshihara, H. Fujihara, Langmuir 15 (1999) 8574.

[7] K. Uosaki, Y. Sato, H. Kita, Langmuir 7 (1991) 1510.

[8] A.C. Templeton, M.J. Hostetler, C.T. Kraft, R.W. Murray, J. Am. Chem. Soc. 120 (1998) 1906.

[9] M.R. Bryce, G. Cooke, A.S. Dhindsa, D. Lorcy, A.J. Moore, M.C. Petty, M.B. Hursthouse, A.I. Karaulov, J. Chem. Soc. Chem. Commun. (1990) 816.

[10] R.R. Schumaker, E.M. Engler, J. Am. Chem. Soc. 99 (1977) 5521.